



Study on the Diagnosis of Rotor Faults in Motors using Inrush Current

Erdenetsetseg SAIJAA¹, Ariunbolor PURVEE^{2*}, Bold ENKHBOLD², Nikita ABRAMOV²

¹*Faculty of Mineral Processing and Engineering, School of Geology and Mining Engineering, Mongolian University of Science and Technology, Mongolia*

²*Faculty of Mechanical and Electrical Engineering, German-Mongolian Institute for Resource and Technology, Ulaanbaatar, Mongolia*

*ariunbolor@gmit.edu.mn

Abstract: Squirrel-cage induction motors are widely used in industry for their durability, simplicity, and cost-efficiency. However, frequent start-stop cycles, overloads, and aging can lead to mechanical and electrical faults, reducing efficiency, causing unplanned downtime, and increasing maintenance costs. Early fault detection is crucial to ensure system reliability and prevent major failures. This study introduces a method for early rotor fault diagnosis by analyzing the stator inrush current during motor startup. Unlike traditional steady-state approaches, this method captures critical fault signatures at energization, enabling earlier and more accurate detection. The approach is validated through lab experiments and dynamic simulations, effectively identifying rotor bar asymmetries and other rotor issues. Additionally, steady-state simulation results complement the transient analysis for a more robust predictive maintenance strategy. A key finding is the identification of a distinct V-line in the Short-Time Fourier Transform (STFT) of the inrush current, serving as a reliable visual indicator of rotor asymmetry. This research is especially important for Mongolia, where motor condition monitoring is underdeveloped. The proposed techniques can be integrated into regular maintenance to extend motor life, reduce downtime, and improve industrial performance.

Keywords: Predictive maintenance, Transient analysis, Fault signature extraction, Dynamic simulation.

1 Introduction

Squirrel-cage induction motors are the cornerstone of industrial operations due to their robustness, simplicity, and cost-effectiveness [1]. They are widely deployed in mining, processing, manufacturing, HVAC, and water pumping applications, especially in countries like Mongolia where industrial infrastructure depends heavily on reliable rotating machinery. Despite their rugged construction, these motors are susceptible to faults caused by frequent start-stop cycles, mechanical wear, voltage imbalance, or thermal stress [2]. Rotor-related faults, in particular, can lead to significant losses if not diagnosed early.

Common rotor faults include broken rotor bars, eccentricity, and cracked end rings, which often begin subtly and worsen over time [3]. Undiagnosed faults can cause reduced efficiency, increased vibration, unplanned outages, and eventual system failure [4]. Therefore, early and accurate fault detection is essential for maintaining operational reliability, reducing maintenance costs, and preventing critical failures in industrial systems.

Traditional fault detection approaches often rely on steady-state Motor Current Signature Analysis (MCSA) or vibration monitoring, both of which have limitations. MCSA is widely used but may not detect incipient faults under light load or noisy operating conditions [5]. Vibration-based methods are effective for mechanical fault diagnosis but require costly sensors

and careful sensor placement [6]. These limitations necessitate the development of more responsive and cost-effective diagnostic techniques.

Transient analysis of inrush current has emerged as a promising approach to overcome these challenges [7][8]. When a motor starts, the initial surge of current—called inrush current—contains rich time-frequency information that reflects the electromechanical state of the motor, including any asymmetries in the rotor. Faults such as broken bars disturb the balance of rotor-induced magnetic fields, leading to detectable distortions in the inrush current waveform [9].

Advanced signal processing techniques, such as the Short-Time Fourier Transform (STFT), Wavelet Transform (WT), and Hilbert-Huang Transform (HHT), have proven useful for extracting fault features from non-stationary signals like inrush current [10], [11]. These approaches enable the detection of faults at the early stages—before they become apparent during steady-state operation.

However, the practical application of inrush current analysis is still limited in many industrial environments due to the need for high-resolution data acquisition systems and complex algorithms [12]. In Mongolia, where industrial motors frequently operate under harsh environmental conditions and where access to advanced diagnostic equipment is limited, systematic research on motor fault detection remains scarce. This study seeks to address that gap by developing and validating a diagnostic methodology based on inrush current analysis, specifically tailored for practical application in both advanced and resource-constrained industrial settings. All validation was carried out at the Motor Repair Center.

2 Inrush Current in Squirrel-Cage Induction Motors: Characteristics and Comparative Study

Inrush current, also known as starting or transient current, refers to the initial surge of current drawn by an induction motor when it is energized. In squirrel-cage induction motors, this current is typically 5 to 8 times higher than the rated current due to the absence of back electromotive force (EMF) at the moment of startup. The magnitude and duration of inrush current depend on several factors including supply voltage, motor design, rotor resistance, and loading conditions.

During startup, the motor rotor is stationary and acts as a short-circuited secondary winding of a transformer. As a result, a large magnetizing current flows into the stator windings, producing substantial electromagnetic torque to overcome inertia. This current gradually decays as the rotor accelerates toward synchronous speed.

Traditionally, inrush current has been viewed as a transient phenomenon that must be minimized or tolerated. However, in recent years, it has been increasingly recognized as a valuable signal for fault diagnosis, especially for early detection of rotor faults such as broken rotor bars, end ring defects, and rotor asymmetry.

Faults in the rotor circuit lead to asymmetries in the magnetic field distribution during startup, which in turn distort the inrush current waveform. Unlike steady-state analysis, inrush current analysis captures these anomalies in their early manifestation, often before they become visible under normal operation. The key features that make inrush current useful for fault detection include:

- High fault sensitivity: ransient conditions magnify the effects of rotor asymmetries.
- Short time window: Startup transients occur in seconds, reducing data collection time.

- _ Independence from load: Fault signatures remain visible even at low or no-load operation.
- _ Ease of measurement: Inrush current can be measured using standard current transformers without interrupting machine operation.

Compared to other diagnostic techniques, inrush current analysis offers distinct advantages for detecting rotor faults in squirrel-cage induction motors. Unlike steady-state MCSA, which shows reduced effectiveness at low load, the inrush method provides reliable fault sensitivity during no-load startup. Relative to vibration and thermal imaging approaches, it requires simpler hardware and is less affected by external disturbances. Although AI-based methods can achieve high diagnostic accuracy, they typically require complex implementation and extensive training datasets. In contrast, inrush current analysis supplies rich, interpretable features directly during motor startup.

Additionally, its short data acquisition period and non-invasive measurement make inrush current analysis practical in both advanced and resource-constrained industrial settings. Taken together, these strengths establish inrush current analysis as a highly sensitive, efficient, and pragmatic diagnostic tool, particularly well-suited for early fault detection and preventive maintenance in critical motor applications.

Versus Steady-State MCSA: Steady-state MCSA is the most widely used electrical diagnostic method. It analyzes sidebands around the fundamental frequency caused by rotor faults. However, its accuracy decreases at low load conditions where slip is minimal and fault components are weak. In contrast, inrush current analysis leverages the higher slip and magnetic asymmetries at startup, yielding stronger fault indicators even under low or no load [13].

Versus Vibration Monitoring: Vibration-based diagnostics are highly sensitive to mechanical faults but require precision sensor placement and can be influenced by external vibrations or structural resonance. Inrush current analysis offers an electrical alternative that is more robust in noisy environments and simpler to implement for rotor-related issues [14].

Versus Advanced AI/ML Approaches: Artificial Intelligence (AI)-based diagnostic systems using machine learning or deep learning provide high diagnostic accuracy but demand extensive training data, computational resources, and system integration. Inrush current analysis can serve as a feature extraction stage in such systems, offering interpretable inputs and reducing model complexity [15].

3 Signal Processing Techniques for Inrush Analysis

The non-stationary nature of inrush current necessitates the use of time-frequency signal processing tools:

- _ Fast Fourier Transform (FFT): Good for steady-state spectral analysis but not ideal for transients.
- _ Short-Time Fourier Transform (STFT): Applies windowed FFT across time, enabling tracking of frequency evolution during startup.
- _ Wavelet Transform (WT): Provides multi-resolution analysis and excels in detecting localized disturbances caused by faults.
- _ Hilbert-Huang Transform (HHT): Effective for adaptive time-frequency representation but computationally intensive.

While inrush current analysis holds great promise, certain challenges remain:

- Need for high-resolution data acquisition: Sampling rates in the range of 10–20 kHz are often required to capture transient signatures.
- Dependence on repeatable startup conditions: Variability in voltage or motor load can introduce noise.
- Interpretation complexity: Fault indicators in transients are often subtle and require expert analysis or automated classification tools.

Future work should focus on integrating machine learning classifiers with inrush current features, developing low-cost transient recorders, and establishing standardized startup protocols for diagnostic consistency.

Inrush current analysis is emerging as a powerful tool for early and reliable rotor fault detection in squirrel-cage induction motors. It addresses key limitations of steady-state techniques and offers enhanced sensitivity, particularly under low-load or transient operating conditions. With continued advancement in signal processing and hardware technology, it is poised to become a key component in next-generation condition monitoring systems for industrial motors.

4 Field Measurements under Rotor Fault Conditions

Field measurements were conducted at the Baganuur coal mine, specifically targeting the cooling fan motors of the dragline excavator model ЭИИ-10/70. The purpose of these measurements was to validate the rotor fault diagnosis methodology under real industrial conditions, using inrush current and electromagnetic torque analysis. The squirrel-cage induction motors assessed during field measurements—7.5 kW, 11 kW, and 22 kW units used for cooling fan operation—are shown in Figure 1.

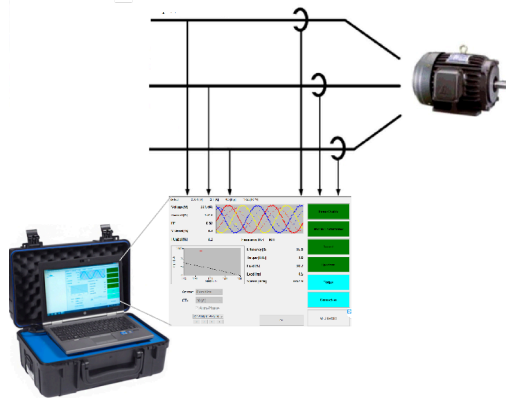


Figure 1: Diagram of measurement in field and labs

To diagnose rotor faults without dismantling the motors, a combination of non-invasive diagnostic tools was employed:

- Phase Sequence Tester (KT8030): Used to verify the correct phase sequence before connecting diagnostic instruments. This ensured that the motors were connected properly to the three-phase supply system. The KT8030 provides visual indicators: a green light for correct phase order and a red light for incorrect connection.

- Infrared Thermometer (SKF T5-600/62 MAX): Used to measure the surface temperature of motors before and during operation. This device detects infrared radiation emitted by heated objects and converts it into visible signals, allowing early identification of abnormal heating. Since equipment typically emits infrared radiation when its temperature rises above zero degrees Celsius, this tool is essential for monitoring the thermal condition of the motors. The SKF T5-600/62 MAX is particularly effective for detecting early-stage overheating due to rotor faults.
- Condition Monitoring System (SKF EXP4000): This high-precision diagnostic device was used for non-invasive evaluation of the motors' electromagnetic torque, voltage, and current characteristics. The EXP4000 enables full-spectrum condition monitoring based on frequency-domain analysis of current and torque signals. It provides a comprehensive picture of motor health by integrating parameters such as electrical load, power quality, and dynamic torque behavior. The SKF EXP4000 is commonly used in global industry and research for condition-based maintenance and motor diagnostics. It is portable, durable, and can operate under low-voltage or battery-powered conditions. It is well-suited for field use in heavy-duty environments such as mining.

The motor diagnostic measurements were carried out by connecting the diagnostic instruments in compliance with safety protocols and proper phase sequencing. The captured data was later analyzed to detect and classify rotor faults. Among these, STFT and WT are most commonly applied in rotor fault diagnosis using inrush current due to their balance between computational effort and accuracy.

The reliable operation of squirrel-cage induction motors is crucial for various industrial applications. However, these motors are susceptible to faults, particularly in the rotor bars, which can significantly affect motor performance and lead to unexpected downtime. To better understand and diagnose rotor faults, controlled field measurements were conducted using motors with varying degrees of rotor damage.

The starting point of the study involved the assessment of a motor operating under normal, healthy conditions. The rotor of this motor, which exhibited no mechanical or electrical faults, is shown in Figure 2. This baseline motor served as a reference to compare and analyze changes in electrical signatures caused by rotor faults during subsequent testing phases.



Figure 2: Motor with no faults

To simulate realistic fault scenarios, rotor bar damages were mechanically introduced in the laboratory environment. The objective was to replicate the different severities of rotor faults that may occur due to manufacturing defects, mechanical wear, or operational stresses such as thermal expansion and mechanical vibrations. This controlled fault induction allowed for a systematic study of the rotor's behavior under varying fault conditions.

The rotor bar damage was created by drilling holes in the rotor bars, a method commonly used to replicate broken bars in experimental setups. The severity of the faults was varied by increasing

the number of drilled holes, as illustrated in Figure 3. The following levels of rotor damage were studied:

- (a) One hole: Representing a minor fault with limited impact on rotor performance.
- (b) Three holes: Indicating a moderate level of damage affecting a larger section of the rotor.
- (c) Six holes: A severe fault condition causing significant degradation in rotor integrity.
- (d) Eight holes: The most extreme fault scenario, simulating extensive rotor bar failure.

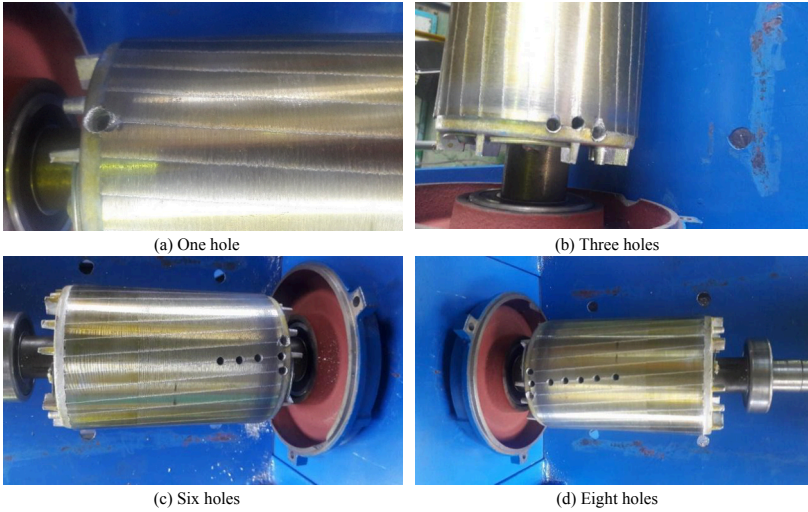


Figure 3: Motor with rotor faults

The laboratory test of the motor was conducted according to the setup shown in Figure 4.

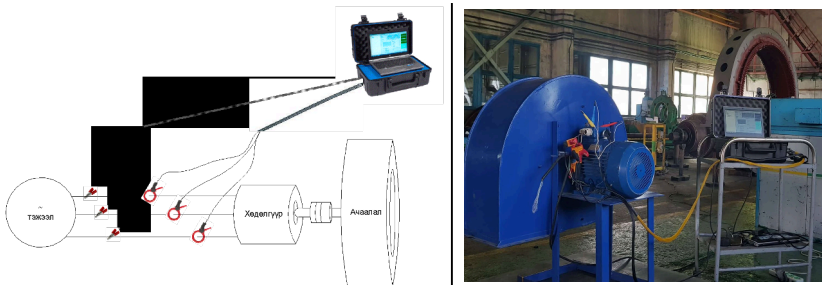


Figure 4: Experimental setup and field study

5 Discussion and Results

Let us consider the algorithm used for analyzing the transient behavior of the motor's electromagnetic torque. When the rotor of an induction motor exhibits asymmetry or faults, a characteristic "V"-shaped curve appears in the instantaneous frequency of the stator current. This V-line the fundamental basis for diagnosing rotor asymmetry or bar faults. The shape and nature of the V-curve are directly influenced by the motor load and electrical parameters.

The instantaneous frequency variation of the stator current is defined as:

$$f_{LSN}(s) = |f_1(1 - 2s)| \quad (1)$$

To obtain the V-line instantaneous frequency line, the Hilbert Transform is applied. The Hilbert Transform is given by:

$$HT(x(t)) = y(t) = \frac{1}{\pi t} \cdot x(t) = \frac{1}{\pi} \int_{-\infty}^{+\infty} \frac{x(\tau)}{t-\tau} d\tau \quad (2)$$

This can be expressed in complex form as:

$$x_a(t) = x(t) + jy(t) = A(t)e^{j\phi(t)} \quad (3)$$

Where:

$$A(t) = [x^2(t) + y^2(t)]^{\frac{1}{2}} \quad \phi(t) = \arctan \frac{y(t)}{x(t)}$$

Using only the real part, the instantaneous frequency is defined as:

$$v_i(t) = \frac{1}{2\pi} \frac{d \arg(x_a)}{dt} = \frac{1}{2\pi} \frac{d\phi}{dt} \quad (4)$$

During motor startup, the motor speed becomes a function of slip frequency, which is given by:

$$s(t) = (\Omega_s - \Omega(t))/\Omega_s \quad (5)$$

Assuming the slip function is quantized in time, a vector of N slip values can be formed. This leads to the generation of two instantaneous frequency curves.

1. The Thevenin equivalent voltage V_{Th} contains the theoretical frequency values corresponding to the calculated slip:

$$v_{Th}[k] = |f_1(1 - 2 \cdot s[k])|, \quad k = 1, \dots, N \quad (6)$$

2. The instantaneous frequency (V-line) calculated from the actual data, denoted as V_{IF} is similarly defined by taking the real part and calculating the phase:

$$v_{IF}[k] = |f_1(1 - 2 \cdot s[k])|, \quad k = 1, \dots, N \quad (7)$$

The correlation between these two curves can be used as an indicator of rotor fault severity. The correlation coefficient is calculated as:

$$Y_{IF} = \frac{cov(v_{Th}, v_{IF})}{\sqrt{cov(v_{Th}, v_{Th}) \cdot cov(v_{IF}, v_{IF})}} \quad (8)$$

The covariance between V_{Th} and V_{IF} is defined as:

$$cov(v_{TR}, v_{IF}) = \frac{1}{N} \sum_{i=1}^N (v_{TR}[i] - \overline{v_{TR}})(v_{IF}[i] - \overline{v_{IF}}) \tag{9}$$

Using these transformations, an algorithm was developed to analyze the transient V-line plot of the motor using the Fast Fourier Transform (FFT), as illustrated in Figure 5.

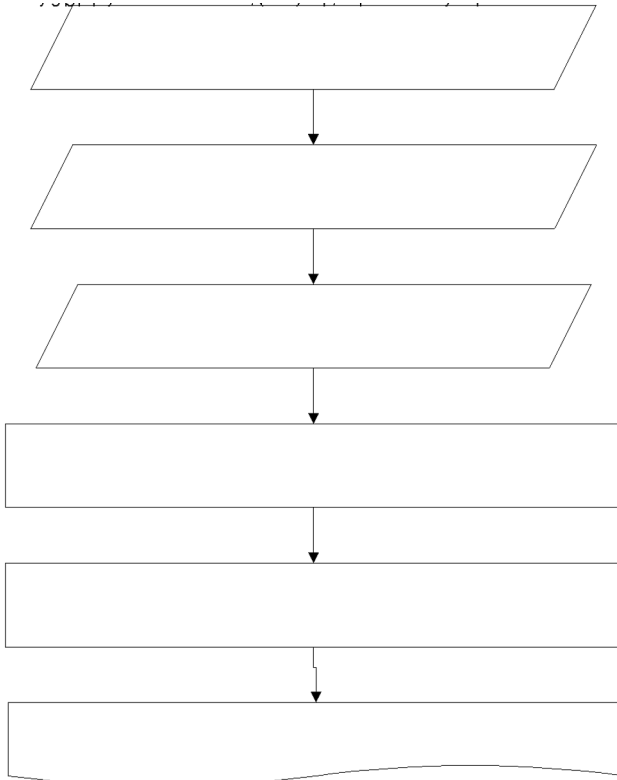
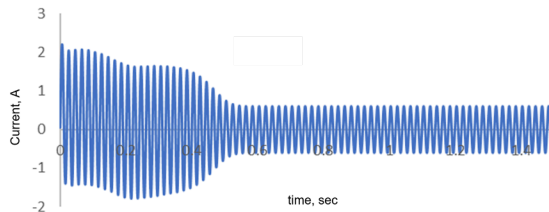


Figure 5: Algorithm of V-line of the motor using the Fast Fourier Transform

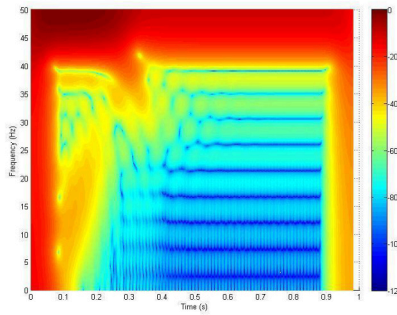
The simulation program based on this algorithm was developed in MATLAB. Motor input parameters were optimized in our previous studies to ensure that the simulated motor outputs closely matched the actual parameters specified on the motor nameplate [16], [17], [18], [19], [20], [21], [22], [23].

The V-line represents a time–frequency spectrogram generated using the Short-Time Fourier Transform (STFT) of the inrush current signal. The color scale of the V-line indicates the signal magnitude (amplitude or power) at each time–frequency point, expressed in decibels (dB). Red / Dark Red indicates a high magnitude (0 to –20 dB), representing dominant frequency components and the strongest signal energy. Yellow / Green indicates a medium magnitude (–20 to –60 dB), representing moderate activity with smaller harmonic or sideband components. Blue / Dark Blue indicates a low magnitude (–80 to –120 dB), representing weak or negligible signal energy.

The transient stator current and V-line of a healthy squirrel cage induction motor, obtained from dynamic simulation, are shown in Figure 6a and Figure 6b, respectively [24] and [25].



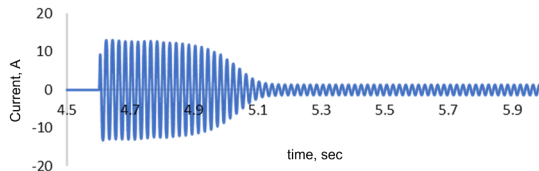
a) Stator current



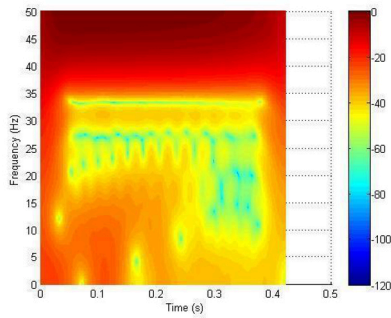
b) V-line in the STFT

Figure 6: Dynamic simulation of a healthy motor

Laboratory-measured transient stator current and its V-line of a healthy motor are illustrated in Figure 7a and Figure 7b, respectively [25].



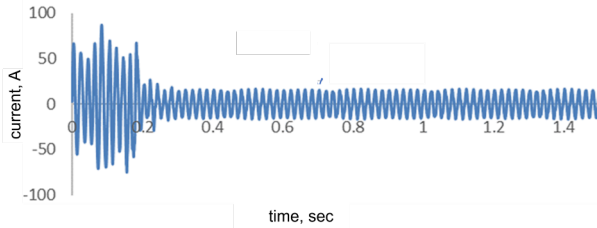
a) Stator current



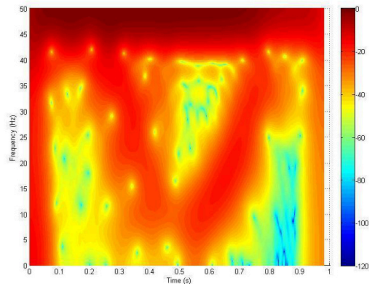
b) V-line in the STFT

Figure 7: Healthy motor in the laboratory.

Figure 8a-b present the simulated motor's stator current and its corresponding V-line for a motor with a rotor bar fault. The V-line is clearly visible [25].



a) Stator current



b) V-line in the STFT

Figure 8: The dynamic simulation with broken rotor bar faults.

Figure 9a-e presents the V-line plots under transient conditions for motors with experimentally induced broken-rotor-bar faults consisting of one, three, four, six, nine, and thirteen drilled holes in the laboratory. These results validate the simulated motors with rotor-bar faults.

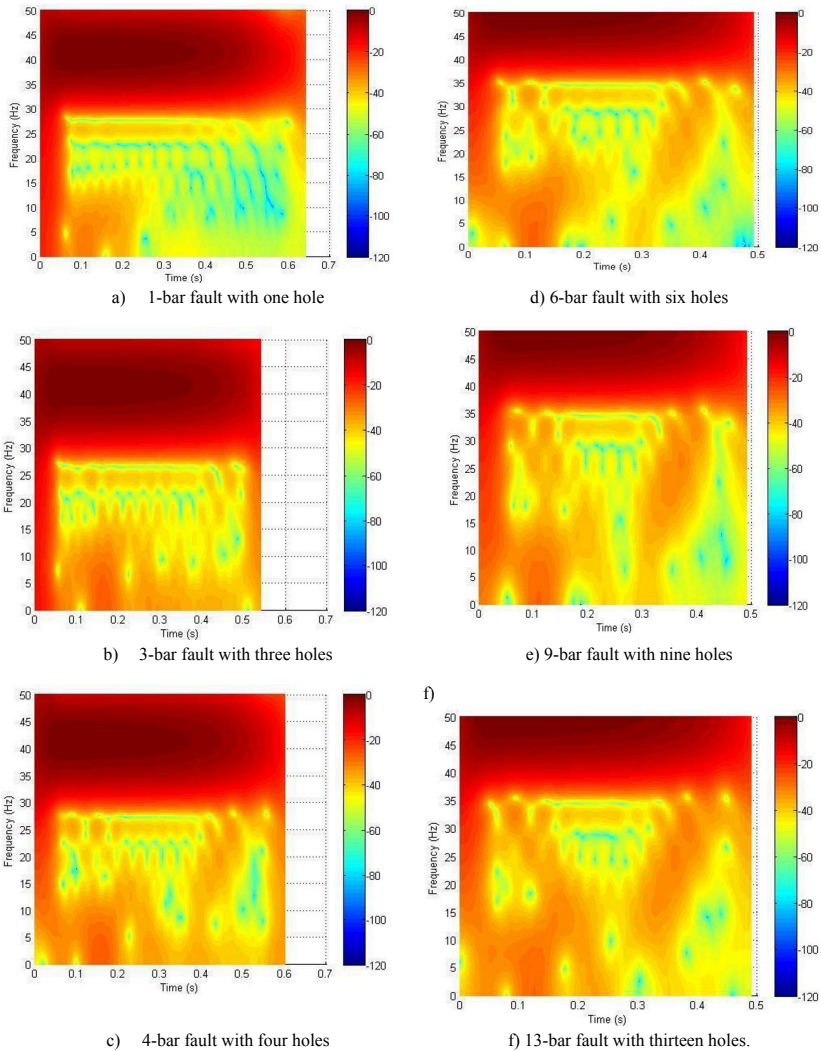


Figure 9: V-line in the STFT of the experimental motor in the laboratory

From Figure 9, the X-axis (Time in seconds) represents the duration of the motor's startup or transient period, while the Y-axis (Frequency in Hz) indicates the frequency content of the stator current. The color scale shows the intensity (magnitude, in dB), where red/yellow corresponds to high magnitude and blue corresponds to low magnitude. In healthy or low-fault motors, the plots typically exhibit a dominant supply frequency component (around the synchronous frequency) with relatively smooth contours. As the number of broken rotor bars increases, however, sideband

frequencies, subharmonics, and oscillations become more pronounced, reflecting higher levels of fault severity.

The subfigures in Figure 9 are explained as follows:

a) 1-bar fault (one hole)

- Only minor distortion is observed, and the V-line is not clearly visible.
- The dominant component remains strong, showing limited impact on motor performance.
- Early signs of rotor asymmetry appear, but they are weak.

b) 3-bar fault (three holes)

- Disturbances become more evident, while the V-line is still indistinct.
- Oscillatory patterns begin to emerge, indicating increased severity.
- Rotor asymmetry becomes more noticeable compared to the 1-bar fault.

c) 4-bar fault (four holes)

- Sideband activity becomes stronger, and the V-line starts to appear.
- The distortion pattern reflects clear mechanical and electrical asymmetry.
- Fault progression is evident with higher disturbance levels.

d) 6-bar fault (six holes)

- Disturbances grow, with multiple bands visible.
- The V-line is now clearly identifiable.
- Motor imbalance increases, and the dominant component weakens compared to early faults.

e) 9-bar fault (nine holes)

- The V-line becomes very distinct, with clear separation of fault-related components.
- Disturbances spread widely, showing strong asymmetry.
- Multiple oscillatory signatures indicate significant rotor damage and instability.

f) 13-bar fault (thirteen holes)

- A severe fault signature is observed, with the V-line clearly visible.
- Widespread distortion dominates the spectrum.
- Strong asymmetry and instability indicate a critical fault condition where motor performance is heavily degraded.

The stator current measurements during the transient operation of a pelletizer motor in an industrial field are shown in Figure 10a, and the corresponding V-line is presented in Figure 10b. From these results, a clear V-line appears in the STFT.

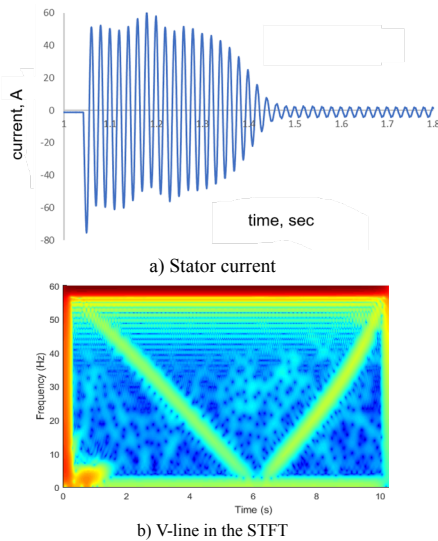


Figure 10: Mill motor of the industry field

The results demonstrate that the V-line serves as a key diagnostic signature for detecting broken rotor bars during motor startup. As the number of broken bars increases, the V-line becomes progressively clearer, reflecting higher levels of rotor damage. This progression from weak or indistinct V-lines (incipient faults) to sharp and well-defined V-lines (severe faults) provides a reliable method for assessing rotor fault severity under transient operating conditions.

6 Conclusion

This study has demonstrated the effectiveness of inrush current analysis as a reliable and sensitive diagnostic method for the early detection of rotor faults in squirrel-cage induction motors. By focusing on the transient startup phase, the proposed approach captures distinct fault signatures—such as rotor bar asymmetries and end-ring defects—that are often undetectable through traditional steady-state analysis techniques. Advanced time-frequency signal processing methods, including the Short-Time Fourier Transform (STFT) and Wavelet Transform (WT), have proven instrumental in extracting these subtle fault indicators from the non-stationary inrush current signals.

Laboratory experiments involving motors with controlled rotor bar damage, along with field measurements conducted under harsh industrial conditions at the Baganuur coal mine, validated the robustness and practical applicability of the method. The results confirm that inrush current analysis not only offers higher fault sensitivity under low- or no-load conditions but also requires simpler and more cost-effective hardware compared to vibration-based or AI-driven diagnostic approaches. This makes it particularly well-suited for industrial environments with limited access to advanced diagnostic tools, such as those found in Mongolia.

A key finding of the study is that the presence of rotor faults is clearly validated by the appearance of a distinct V-line in the STFT of the motor's inrush current. This V-line serves as a

reliable visual indicator of rotor asymmetry, making it a powerful diagnostic signature for early fault detection.

Furthermore, this research highlights the value of transient condition monitoring in complementing steady-state diagnostics, enabling a more comprehensive assessment of motor health. It facilitates predictive maintenance strategies that can extend motor lifespan, reduce unplanned downtime, and enhance overall operational efficiency.

In summary, the developed diagnostic methodology based on inrush current analysis represents a practical, accurate, and cost-effective solution for rotor fault detection in squirrel-cage induction motors. Its integration into routine maintenance programs has the potential to significantly improve industrial reliability and productivity, addressing a critical gap in motor condition monitoring both locally and globally. Future work will focus on integrating machine learning algorithms to automate fault classification and on developing standardized protocols to further enhance diagnostic consistency and usability.

ACKNOWLEDGEMENT

The authors gratefully acknowledge the German-Mongolian Institute of Resources and Technology (GMIT) for providing the opportunity to present and publish this research paper. Additionally, the authors extend their sincere appreciation to Mon-Tsahim Motor Repair Center for granting access to facilities and support necessary to conduct the experimental work.

REFERENCES

- [1] M. El and H. Benbouzid, "A Review of Induction Motors Signature Analysis as a Medium for Faults Detection," *IEEE TRANSACTIONS ON INDUSTRIAL ELECTRONICS*, vol. 47, no. 5, pp. 984–993, Oct. 2000.
- [2] Peter Vas, *Parameter Estimation, Condition Monitoring and Diagnosis of Electrical Machines*, 1st ed. University of Aberdeen, United Kingdom: Clarendon Press, Oxford, 1993.
- [3] A. Bellini, F. Filippetti, C. Tassoni, and G. A. Capolino, "Advances in diagnostic techniques for induction machines," *IEEE Transactions on Industrial Electronics*, vol. 55, no. 12, pp. 4109–4126, 2008, doi: 10.1109/TIE.2008.2007527.
- [4] R. Supangat, J. Grieger, N. Ertugrul, W. L. Soong, D. A. Gray, and C. Hansen, "Detection of broken rotor bar faults and effects of loading in induction motors during rundown," in *Proceedings of IEEE International Electric Machines and Drives Conference, IEMDC 2007*, 2007, pp. 196–201. doi: 10.1109/IEMDC.2007.383576.
- [5] A. Siddique, G. S. Yadava, and B. Singh, "A review of stator fault monitoring techniques of induction motors," *Mar. 2005*, doi: 10.1109/TEC.2004.837304.
- [6] A. M. Trzynadlowski, "Detection of Mechanical Abnormalities in Induction Motors by Electric Measurements," *International Journal of Rotating Machinery*, vol. 5, no. 1, pp. 41–52, May 1999.
- [7] M. A. Awadallah and M. M. Morcos, "Application of AI tools in fault diagnosis of electrical machines and drives - An overview," *Jun. 2003*. doi: 10.1109/TEC.2003.811739.
- [8] S. Nandi, H. A. Toliyat, and X. Li, "Condition monitoring and fault diagnosis of electrical motors - A review," *Dec. 2005*. doi: 10.1109/TEC.2005.847955.
- [9] Moutaz Bellah Benrad, Adel Ghoggal, Tahar Bahi, and Seif Eddine Bouziane, "Fault detection of induction machine using artificial neural networks," *2024 8th International Conference on Image and Signal Processing and their Applications (ISPA)*, pp. 1–7, Jun. 2024.
- [10] K. Kim and A. G. Parlos, "Induction motor fault diagnosis based on neuropredictors and wavelet signal processing," *IEEE/ASME Transactions on Mechatronics*, vol. 7, no. 2, pp. 201–219, Jun. 2002, doi: 10.1109/TMECH.2002.1011258.
- [11] A. Medoued, A. Lebaroud, and D. Sayad, "Application of Hilbert transform to fault detection in electric machines," *Adv Differ Equ*, vol. 2013, 2013, doi: 10.1186/1687-1847-2013-2.
- [12] J. Faiz and B. M. Ebrahimi, "A new pattern for detecting broken rotor bars in induction motors during start-up," *IEEE Trans Magn*, vol. 44, no. 12, pp. 4673–4683, Dec. 2008, doi: 10.1109/TMAG.2008.2002903.
- [13] A. Guedidi and W. laala, "Novel Rotor Fault Diagnostic Method Based on RLMD and HT Techniques," in *The 10th International Conference on Computer Science and Information Technology (CSTY 2024)*, David C. Wyld et al., Ed., Toronto, Canada: Academy and Industry Research Collaboration Center (AIRCC), Jul. 2024, pp. 17–26. doi: 10.5121/csit.2024.141302.
- [14] V. Biot-Monterde, A. Navarro-Navarro, I. Zamudio-Ramirez, J. A. Antonino-Daviu, and R. A. Osornio-Rios, "Automatic Classification of Rotor Faults in Soft-Started Induction Motors, Based on Persistence Spectrum and

- Convolutional Neural Network Applied to Stray-Flux Signals,” *Sensors*, vol. 23, no. 1, Jan. 2023, doi: 10.3390/s23010316.
- [15] U. Ali, W. Ali, and U. Ramzan, “An Improved Fault Diagnosis Strategy for Induction Motors Using Weighted Probability Ensemble Deep Learning,” <https://www.researchgate.net/publication/387382886>. [Online]. Available: <http://arxiv.org/abs/2412.18249>
- [16] “Ariunbolor Purvee, “Code of Grey Relational Analysis”.
- [17] A. Purvee, “Code of Grey Relational Analysis,” MATLAB Central File Exchange. [Online]. Available: <https://tinyurl.com/y6fjewbfz>
- [18] Ariunbolor Purvee, “Gui for Grey Relational Analysis.pdf,” MATLAB Central File Exchange. [Online]. Available: <https://tinyurl.com/y6fjewbfz>
- [19] Ariunbolor Purvee, “Dynamic simulation and Simulation of Squirrel Cage Induction Motor,” Thesis, Mongolian University of Science and technology, Ulaanbaatar, 2009.
- [20] A. Purvee and I. Member, “Optimal Parameters Determination of Simulated Motors Based on Orthogonal Arrays,” pp. 4–9.
- [21] A. Purvee and O. Choidorj, “Determination of Combination of Input Values of Simulated Motor Using Taguchi Method,”
- [22] A. Purvee and O. Choidorj, “Optimization of Input Values of Simulated Motors Using Grey Relational Analysis,” in *the 3rd International Conference on Electrical, Communication and Computer Engineering (ICECCE)*, Kuala Lumpur: IEEE, Jun. 2021, pp. 12–13.
- [23] A. Purvee and O. Choidorj, “Optimization of Input Values of Simulated Motors Using Grey Relational Analysis,” 2021.
- [24] Ц. ЭНХБАТ, “Асинхрон хөдөлгүүрийн роторын гэмтлийг доргионы ба цахилгаан соронзон моментын үл задлах аргаар оношлох судалгаа,” Диссертаци, Шинжлэх ухаан технологийн их сургууль, 2019.
- [25] Нансалын Уянга, “Уурхайн цахилгаан хөдөлгүүрийн роторын гэмтлийг гүйдлийн үл задлах аргаар оношлох судалгаа,” магистрын ажил, ШУТИС, Улаанбаатар, 2021.

Open Access This chapter is licensed under the terms of the Creative Commons Attribution-NonCommercial 4.0 International License (<http://creativecommons.org/licenses/by-nc/4.0/>), which permits any noncommercial use, sharing, adaptation, distribution and reproduction in any medium or format, as long as you give appropriate credit to the original author(s) and the source, provide a link to the Creative Commons license and indicate if changes were made.

The images or other third party material in this chapter are included in the chapter's Creative Commons license, unless indicated otherwise in a credit line to the material. If material is not included in the chapter's Creative Commons license and your intended use is not permitted by statutory regulation or exceeds the permitted use, you will need to obtain permission directly from the copyright holder.

